The University of Tehran Press

Pollution

https://jpoll.ut.ac.ir/

Print ISSN: 2383-451X
Online ISSN: 2383-4501

Selective Nickel and Chrome Ions Adsorption from Aqueous Solutions using Phycocyanin-Functionalized Magnetic Nanosorbent

Kimia Imani | Alireza Habibi✉ | Shadi Azar

Chemical Engineering Department, Faculty of Engineering, Razi University, Kermanshah, Iran

Article Info

Article type:
Research Article

Article history:
Received: 4 Apr 2026
Revised: 9 Jun 2026
Accepted: 5 Sep 2026

Keywords:
Phycocyanin,
Magnetic nanoparticles,
Nanosorbent,
Pseudo-second-order model,
Langmuir isotherm

ABSTRACT

Contamination of water resources to heavy metals is a crucial environmental concern due to its toxicity effects on ecosystems and human health. This study focuses on the development of an efficient green nanosorbent for the selective adsorption of Ni (II) from Cr (VI) ions in aqueous solutions using phycocyanin-functionalized magnetic nanosorbents (PC-nanosorbent). This approach gains a potential for the recovering of these heavy metals from industrial effluents and reuse them. The adsorption experiments revealed a monolayer adsorption carried out between the ions and functional groups in the nanosorbents. The PC-nanosorbent showed higher efficiency for Ni(II) removal whereas Cr(VI), confirming a selective adsorption of these metals. Kinetic modeling indicated that the pseudo-second-order model best described the adsorption processes of these metals on the PC-nanosorbents, and a faster adsorption kinetics for Ni(II) compared to Cr(VI) was observed. Also, the Langmuir adsorption coefficients were q_{max} = 19.16 mg g^{-1} and K_L = 0.0023 L mg^{-1} for Ni (II), and q_{max} =14.45 mg g^{-1} and K_L = 0.2039 L mg^{-1} for Cr (VI). Furthermore, regeneration tests over three cycles showed good reusability, with a maximum capacity decrease of 16%. The results of this study indicate the potential of magnetic nanosorbents as a selective, efficient, feasible, and reusable technique for the selective adsorption of nickel from chromium ions in aqueous environments.

Cite this article: Imani, K., Habibi, A., & Azar, S. (2026). Selective Nickel and Chrome Ions Adsorption from Aqueous Solutions using Phycocyanin-Functionalized Magnetic Nanosorbent. *Pollution*, 12(3), 784-798. https://doi.org/10.22059/poll.2026.407588.3221

DOI: https://doi.org/10.22059/poll.2026.407588.3221

INTRODUCTION

Heavy metal ions including nickel (Ni (II)) and chromium (Cr (VI)) enter the environment through both natural and human activities. Natural sources include volcanic eruptions, soil erosion, and weathering of rocks. Human activities, particularly industrial processes, contribute significantly to their release. These processes include mining, smelting, manufacturing (especially electroplating and leather tanning), and even waste disposal. Furthermore, agricultural activities, like the use of certain fertilizers, can also introduce these metals into the environment (Tchounwou et al., 2012). Both Ni (II)) and Cr (VI) are toxic that pose significant threats to human health and ecosystems where Cr (VI) is a known human carcinogen (Sable et al., 2024). Therefore, the removal of these metal ions from industrial wastewater is essential. The heavy metal removal approaches mainly include precipitation, adsorption, ion exchange, electrodialysis, and membrane processes; however, membrane technologies, adsorption, and ion exchange are of particular interest to researchers (Thiripelu et

*Corresponding Author Email: *a.habibi@razi.ac.ir*

al., 2024). Adsorption is especially attractive due to its simplicity, low cost, and high efficiency. It is supported by a strong scientific and experimental foundation. Additionally, its recyclability and reusability make it an economical and viable method (Yi et al., 2025).

Biological adsorption as a green approach applies biomaterials such as bacteria, fungi, algae, and agricultural residues to immobilize various metals from aquatic environments via creating complexes between metals and the specific groups in biomaterials (Tabish et al., 2024). Previous findings indicate cyanobacteria play a vital role in removal of heavy metals due to their unique composition of their cell walls having a relatively high surface area with high affinity to metal ions (Hossain and Okino, 2024). Furthermore, the application of non-living cells of cyanobacteria as the biological adsorbent of various heavy metals has been investigated (Shinde et al., 2008). It indicates the functional groups participating in the adsorption of heavy metals for both living and non-living cyanobacteria cells are mainly the same. Therefore, the removal of heavy metal ions by cyanobacteria cells may have occurred through a passive adsorption mechanism (Li et al., 2021). Further investigations on cyanobacteria cells showed that phycocyanin (PC), a natural pigment produced by cyanobacteria, has high intensity to formation of complex with metal ions (Thevarajah et al., 2023). PC is composed of a protein and a non-protein component known as phycocyanobilin (PCB). PCB is an open-chain tetrapyrrole responsible for the intense blue color of PC (Fernández et al., 2014).

Nitrogen-rich polymers are new and promising materials for removing heavy metal ions, because nitrogen centers strongly favor the direct adsorption of heavy metal ions. One of these polymers, polypyrrole (PPy), has been investigated because of its great redox reversibility, and environmental stability. Nevertheless, these conductive polymers tend to aggregate in water because of π–π interactions, limiting the amount of accessible active sites. This results in limited dispersion, making it more difficult to remove heavy metal ions. As a result, the rational functionalization of conducting polymers with amine-containing groups is a useful way to overcome these drawbacks by increasing the hydrophilicity and number of accessible adsorption sites that raise the potential for heavy metal ions adsorption. (Motawea et al., 2024). Polyethyleneimine (PEI) is a water-soluble polymer containing plenty of primary and secondary amino groups on the chain, which is frequently used to modify adsorbents by grafting onto supporting materials to improve their adsorption capacity for heavy metals (Zhang et al., 2026). In past research, (PPy)-based adsorbents have played an important role in the removal of various heavy metals (Muhammad et al., 2016). The binding of heavy metals to phycocyanin has also been investigated and proven in previous studies and they have used this property to prepare various sensors and devices to detect the presence of heavy metals in small quantities (Gelagutashvili et al., 2013; Bellamy-Carter et al., 2022). Previously, an immobilized PC on rice hull nano silica using 3-aminopropyltriethoxysilane (APTES) and glutaraldehyde as the crosslinking agent was used for cadmium removal from aqueous media (Sinad et al., 2021).

The progress in synthesis of Fe_3O_4 magnetic nanoparticles (MNPs) has been an opportunity in the development of efficient adsorbents in the last decades (Alyasi et al., 2025; Paryav et al., 2025). These magnetic adsorbents could efficiently be dispersed in aqueous medium during the process and then easily separated along with the adsorbed pollutants using an external magnet (Karami et al., 2024). Previous findings showed that metal ions can chelate with amine groups (Wang et al., 2006, Anfar et al., 2020). Polyethyleneimine (PEI) as a branched hydrophilic macromolecule with abundant amine functional groups was extensively applied for the preparation of amino-functionalized Fe_3O_4 nanoparticles (Chen et al., 2015; Ayalew at al., 2022; Bagdat et al., 2023). PEI has also been used in past research to remove heavy metals (Ayalew et al., 2022). Although the nanosorbents are efficient in removal of metal ions, they did not show a selective adsorption for the heavy metal ions. The aim of the present study was

the application of PC as a natural structure containing tetrapyrrole rings in the development of a magnetic PEI-nanosorbent for selective adsorption of Ni (II) from Cr (VI) from aqueous solutions. The adsorption experiments were performed at different initial concentrations and the obtained isotherms were compared with the Langmuir model. Also, the kinetics modeling was performed to evaluate the rate of the adsorption processes by the PC-nanosorbent. The novelty of this work lies in the synthesis of a novel hybrid nanosorbent by co-functionalizing Fe_3O_4nanoparticles with both PEI and purified PC. Unlike previous studies that utilized either whole biomass cells (suffering from diffusion limits) or single-modified PEI@ Fe_3O_4(lacking specific binding sites), this study combines the high density of amine groups from PEI with the unique coordination chemistry of PC. This dual-functionalization strategy creates a synergistic effect that not only overcomes the mass transfer barriers associated with intact cells but also provides specific active sites for enhanced metal immobilization, distinguishing it from conventional PEI-based or unmodified biomolecule adsorbents.

MATERIAL AND METHODS

Dried powders of PC (extracted from *Spirulina platensis*) and *Spirulina* dried powder were obtained from Bio Green Company (Iran). Potassium dichromate ($K_2Cr_2O_7$), nickel nitrate ($Ni(NO_3)_2$), dipotassium hydrogen phosphate (K_2HPO_4), mono-potassium phosphate (KH_2PO_4), hydrochloric acid (HCl), and sodium hydroxide (NaOH) were also obtained from Merck (Germany).

To prepare phycocyanin-functionalized nanosorbent (PC-nanosorbent), 2 g of Fe_3O_4 MNPs were initially mixed with a PEI solution at 0.5% wv^{-1} and agitated for 24 h at 30 °C and 150 rpm (Ayalew et al., 2022). The obtained activated nanoparticles (PEI@ Fe_3O_4) were separated using filter paper and then dried in a vacuum oven at 30 °C for 24 h. Next, the PEI@ Fe_3O_4 nanoparticles were added to 50 mL of a 10% wv^{-1} of PC solution and the mixture was mixed in a shaker incubator at 30 °C and 150 rpm for 24 h. The obtained PC-nanosorbent particles were separated using filter paper and then dried in a vacuum oven at 30 °C overnight. The process schematic is shown in Figure 1. The Fourier-transform infrared (FTIR) analysis in the range of 4000–400 cm^{-1} was used to identify the characteristic functional groups during the synthesis of the PC-nanosorbent.

Also, to investigate the amount of phycocyanin adsorbed on the nanosorbent, an UV-Vis spectrophotometer was used to determine the identifying absorbance peaks of the C-PC solutions as 652, and 620 nm. Then, the concentration of C-PC (C, mg mL^{-1}) in the solution, before and after being exposed to nanoparticles, was estimated as follows: (Hu et al., 2024):

$$C = \frac{A_{620} - 0.477 A_{652}}{5.34} \quad (1)$$

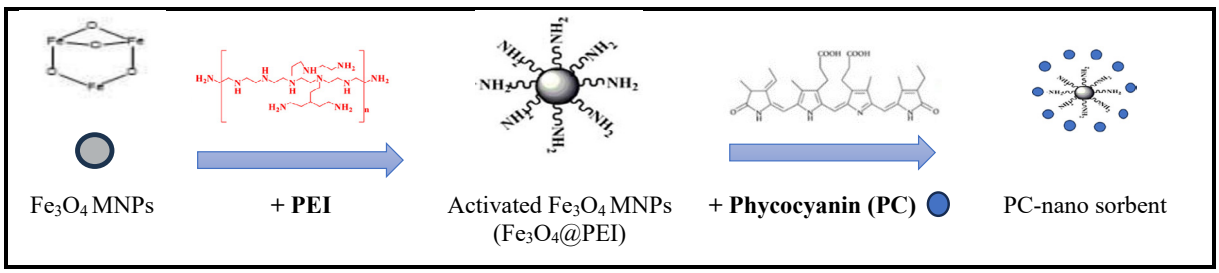

Fig. 1. Schematic view of the procedure used for the PC-nano-adsorbent preparation.

The performance of the PC-nanosorbent in the removal of Ni (II) and Cr (VI) ions was comparted with dry *Spirulina* powder, PEI@ Fe_3O_4, and raw Fe_3O_4 MNPs. In the experiments, 0.2 g of the adsorbent sample was added to 15 mL of Ni (II) or Cr (VI) solution with an initial concentration of 200 mg L^{-1} in 50 mL Erlenmeyer flasks. All solutions were prepared using a phosphate buffer (1 M and pH = 7) (Musah et al., 2022). The adsorption process was carried out under 30 ± 1 °C and 150 rpm for 24 hours in a shaker incubator. After this period, the immobilization yield (Y) and adsorption capacity (q) were determined using the following formula (Chen et al., 2014, Dube et al., 2016):

$$Y(\%) = 100 \times \frac{C_0 - C_f}{C_0} \tag{2}$$

$$q\left(\text{mg g}^{-1}\right) = \frac{V \times \left(C_0 - C_f\right)}{m} \tag{3}$$

Where C_0 is the initial concentration of metal in the solution (mg L^{-1}), C_f is the final concentration of metal in the solution after the adsorption experiment (mg L^{-1}). Also, V (L) and m (mg) are the volume of the solution and mass of the adsorbent, respectively.

To investigate the effect of pH in the adsorption process, the standard solutions of Ni (II) and Cr (VI) with an initial concentration of 200 mgL^{-1} were adjusted to pH level of 5.5 and 8.0. The levels of pH were selected based on the previous works that showed PC is stable in pH range from 5 to 8 (Antelo et al., 2008, Ebrahimi et al., 2023).

To investigate the competitive effects of Ni (II) and Cr (VI) ions during the adsorption experiments, the above experiments were repeated in the presence of 200 mg L^{-1} of both Ni (II) and Cr (VI) ions.

The adsorption kinetics of Ni (II) and Cr (VI) ions was also determined by the measurement the temporal variation of these metals in the aqueous phase where the initial concentration of Ni (II) or Cr (VI) was 500 mg L^{-1} (Gelagutashvili and Tsakadze, 2013). Also, the adsorption process on the PC-nanosorbent at different initial concentration of these ions ranging from 25 mg L^{-1} to 1000 mg L^{-1} were performed and the steady state experimental values (after 24 h) were fitted to the Langmuir isotherm model with following expression:

$$q_e = \frac{q_{\max} \times K_L \times C_e}{1 + K_L \times C_e} \tag{4}$$

where, q_e (mg g^{-1}) is the amount of metal adsorbed at equilibrium, C_e (mg L^{-1}) is the equilibrium concentration of the metal ion in solution, q_{max} (mg g^{-1}) represents the maximum adsorption capacity, and K_L (L mg^{-1}) is the Langmuir constant related to the affinity of the binding sites.

The reusability of PC- nanosorbent was checked according to the previous works (Chen et al., 2014, Benettayeb et al., 2021). The spent PC-nanosorbent that previously used for Cr (VI) immobilization were placed in water with an adjusted pH = 8 using 0.5 N NaOH solution and then agitated at 200 rpm for 30 min. After this period, the PC-nanosorbents were separated by an external magnet and then dried in a vacuum oven at 30 °C for 24 hours. For nanosorbent particles that previously used for nickel adsorption, the same process was done, however the pH was set on 5.5 using a 0.5 N HCl solution for desorption of Ni (II) ions. The recovered nanosorbents were then used for the next adsorption cycles.

The concentration of metals in all test solutions was measured by the atomic absorption. All adsorption experiments were conducted triplicate and the mean values ± errors were reported.

RESULTS AND DISCUSSION

The efficiency (*Y* (%)) and adsorption capacities (q (mg g^{-1})) of the PC-nanosorbent for the adsorption of Ni (II) and Cr (VI) ions from aqueous solutions is compared with *Spirulina* powder, raw Fe_3O_4 MNPs and PEI@Fe_3O_4 MNPs in Figure 2. The microalgae cells could be immobilized 64% and 30.8% of Ni (II) and Cr (VI) ions, respectively. Raw Fe_3O_4 MNPs also removed 20 of Ni (II) and 15% of Cr (VI) ions from the aqueous media. PEI@Fe_3O_4 MNPs due to the presence of amino groups were more efficient in the adsorption of ions and removed up to 73 % of Ni (II) and 30.67 % of Cr (VI). However, the PC-nanosorbent developed in the present study were respectively enhanced the immobilization yields of Ni (II) and Cr (VI) ions by 13.7% and 4.89 % at the same experimental conditions. Therefore, the PC-nanosorbent could remove the main part of the initial Ni (II) ions (83%) from the aqueous environment while the Cr (VI) ions partially attached to this adsorbent (32.17%). However, the adsorption capacity of the PC-nanosorbent was 29.69 % higher than *Spirulina platensis* for the adsorption of Ni (II) ions and value of *q* reached to 12.45 mg g^{-1}. The results of Figure 2, also indicate that the removal yield and efficiency for Ni (II) were higher than Cr (VI) ions for all test adsorbent systems. It is in agreement with the previous findings indicate Ni (II) ions due to a smaller hydrated radius and stronger electrostatic interactions with the amine groups could be efficiently attached to amino-functionalized adsorbent particles (Bagdat et al., 2023). While, Cr (VI) ions mainly found in chromate and dichromate anionic forms has higher hydrated radius and it decreases their affinity to the adsorbent into the surface of positive charge groups.

As can be seen in the results, the presence of phycocyanin increased the absorption of heavy metals by increasing the number of heavy metal acceptor sites. However, this increase was greater for Ni (II). In one study, an adsorbent containing polypyrrole and glycine (PPy-gly adsorbent) was used to remove Cr (VI). The adsorption of Cr (VI) onto the PPy-gly adsorbent was highly pH dependent and removal efficiency by PPy-gly was much higher compared to PPy homopolymer. They showed that the mechanism of chromium adsorption was through binding to the amino group of glycine (Ballav et al., 2012). Since Cr (VI) has a lower affinity for binding to pyrrole rings, in our study, the addition of phycocyanin to the adsorbent probably limited the amine branches of PEI, resulting in less chromium being adsorbed.

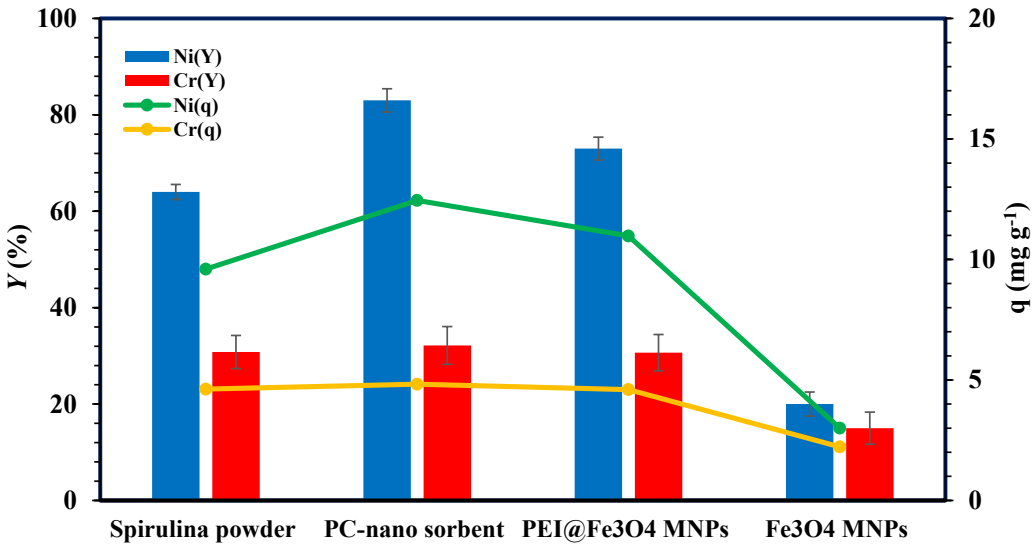

Fig. 2. The immobilization yield and adsorption capacity for the immobilization of Ni (II) and Cr (VI) form aqueous solutions.

In one study, a novel microcrystalline cellulose-based adsorbent MCC@$CaCO_3$/LPEI was synthesized via a facile precipitation reaction, and used for the separate and simultaneous removal of Cd (II), Pb (II), Cr (VI), Cu (II), and Zn (II) from aqueous solution. Results showed that MCC@CaCO3/LPEI could remove 99.2 - 99.9 % of low-level heavy metals (1–2 mg L^{-1}) in the mono-component system (Zhang et al., 2026). Previously, the application of the rice hull nano silica activated by the PC provided higher cadmium adsorption efficiency (82.47%) against the bare rice hull nano silica (79.28%), with an initial concentration of 0.5 ppm, where the adsorption capacity was 19.72 ± 0.38 mg g^{-1} (Sinad et al., 2021). The effect of the presence of phycocyanin in our results is higher, while the initial concentration of heavy metal was also much higher. To our knowledge, there is no other study on this subject.

The efficiency and adsorption capacities of the adsorbents in the simultaneous presence of Ni (II) and Cr (VI) ions was also evaluated and the results are presented in Figure 3. A comparison of the Ni (II) and Cr (VI) immobilization yields in Figure 2 and 3 showed the performance of *Spirulina platensis* for both ions immobilization is same in single and double presence of the ions in the aqueous system. However, the performance of the nanosorbents slightly decreased for Ni (II) adsorption in the simultaneous presence of the ions. The results also indicates that the application of phycocyanin layer in the PC-nanosorbent caused to increase in the removal yield of Ni (II) against Cr (VI) in the simultaneous presence of ions. This confirmed the role for surface modification and functional groups in PC-nanosorbent for a selective adsorption of metal ions. This finding is appropriate for treating of real wastewaters where the nickel and chrome ions simultaneously presented. The higher removal efficiency of Ni (II) compared to Cr (VI) is mainly related to the specific chemical nature of phycocyanin, rather than just a simple increase in surface area. Phycocyanin contains various functional groups such as amines and carboxyls (Fernández-Rojas et al., 2014). These groups may interact more strongly with Ni (II) ions through coordination bonds. On the other hand, Cr (VI) usually exists as negative ions (anions) in the solution. Since the amine groups on the adsorbent surface are often positively charged at lower pH, there might be some electrostatic repulsion or weaker interaction for Cr (VI). Additionally, the structure of the phycocyanin protein might allow smaller Ni (II) ions to

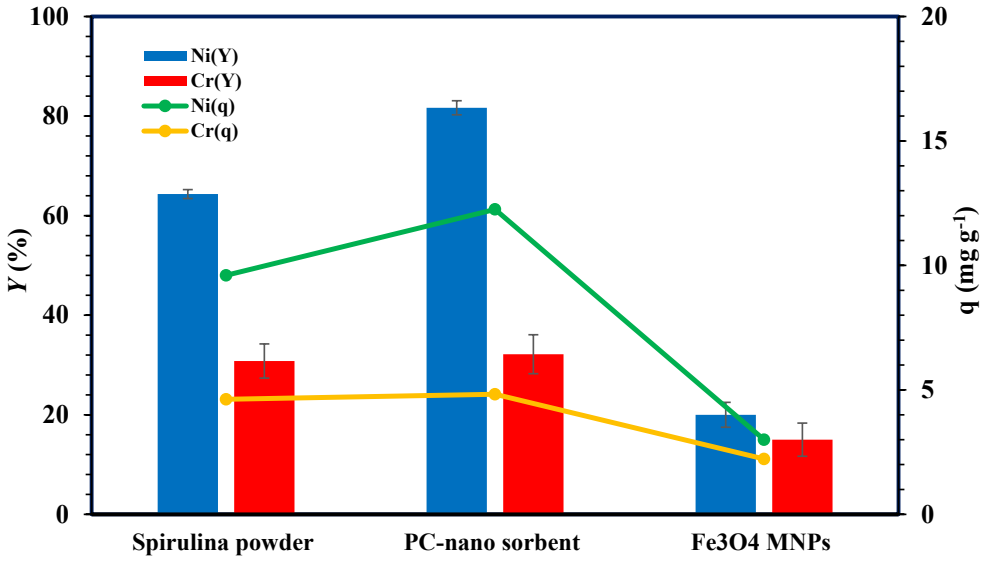

Fig. 3. The immobilization yield and adsorption capacity in the experiments with simultaneous presence of Ni (II) and Cr (VI) in aqueous solutions.

access binding sites more easily than larger Cr (VI) ions. Therefore, it seems that phycocyanin helps in selectively targeting Ni (II) over other ions.

UV-VIS absorption measurements showed that 25 mg of phycocyanin in the solution was adsorbed by the 2 g of PEI@Fe_3O_4 MNPs. The FTIR spectrum could provide crucial facts of the functional groups in the PC-nanosorbent that participate in the adsorption of Ni (II) and Cr (VI) ions. Figure 4 shows the FTIR spectra of the samples during the synthesis of PC-nanosorbent. In the spectrum corresponding to Fe_3O_4 MNPs, the large broad band at 3400 cm^{-1} related to the –OH stretching vibration. The absorption picks were around 1620 cm^{-1} due to the symmetric and asymmetric bending vibration of C=O. The strong band between 500 and 700 cm^{-1} are assigned to Fe-O stretching mode and iron (II) oxide stretching. These results are also consistent with those obtained in previous research (Sobhanardakani et al., 2018). Adsorption in the wave numbers of 1568.2, 1475.44, 1313.43 cm^{-1} indicated the presence of N-H bond in primary, secondary and tertiary amines, respectively (Kazazi et al., 2013). The FT-IR spectrum of PEI@ Fe_3O_4 MNPs reveals a peak at around 1621 and 1385 cm^{-1} indicated the presence of N-H. The FT-IR spectrum of the phycocyanin reveals a peak at around 1600–1500 cm^{-1} is attributed to the C–N stretching and N–H bending vibrations. Also, the stretching vibration of the C=O bond at 1700–1600 cm^{-1}. The presence of C–H vibrations is identified at the 2890–2980 cm^{-1} region. The broad peak at 3315 cm^{-1} is related to the –OH stretching vibrations (Hu et al., 2024). Peaks in the range 980-1140 are related to pyrrole rings (Muhammad et al., 2016). It can be seen that the PC-nanosorbent has characteristic peaks at 3414, 1619.81, 1390.25, and 623.53 cm^{-1}. The peak at 3414 cm^{-1} corresponds to –OH bonds. The peak at 1619.81 cm^{-1} is attributed to C=O stretching. The peak at 1390.25 cm^{-1} indicates $–COO^-$ or CH bending, while the peak at 623.53 cm^{-1} corresponds to Fe–O vibrations in the Fe_3O_4 MNPs. These results confirm the successful functionalization of the magnetic adsorbent with phycocyanin. Indeed, the coexistence of both organic (–OH, –NH, C=O, $–COO^-$) and inorganic (Fe–O) bands shows the successful coating of phycocyanin onto the magnetic particles and suggests the availability of multiple active sites

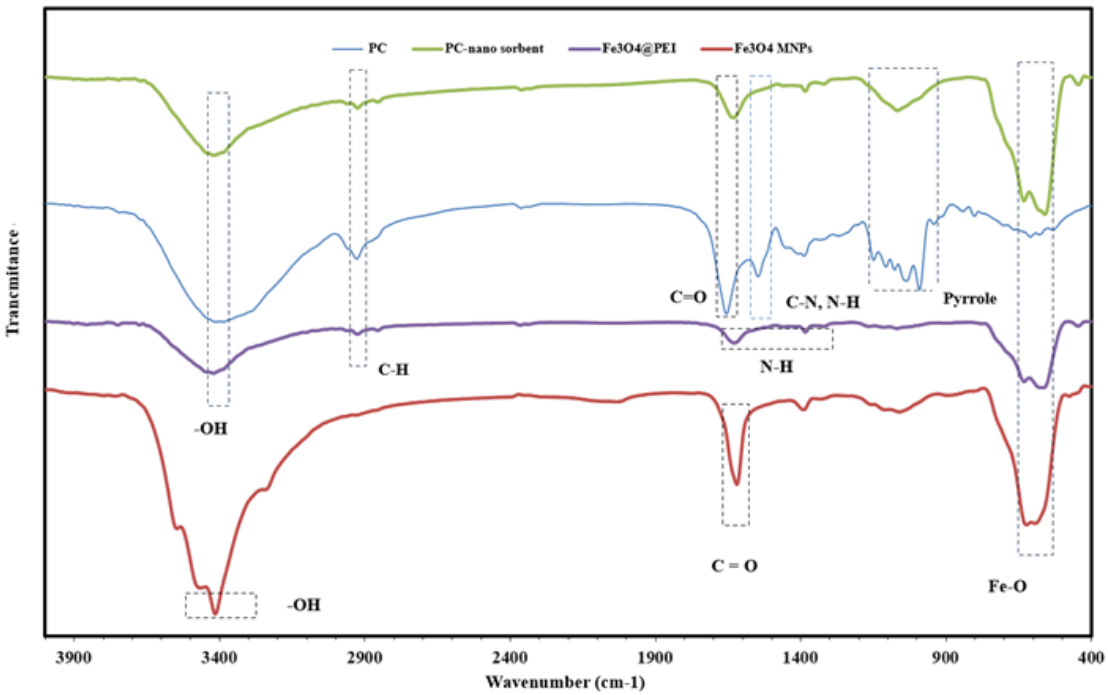

Fig. 4. FTIR spectrums for the samples during the synthesis of the PC-nano sorbent particles.

for heavy metal binding. Peaks in the range of 980-1140 corresponding to pyrrole rings also confirm the presence of phycocyanin in PC-nanosorbent. There is no peak in this region in the Fe_3O_4@PEI before PC attachment. The decrease in peak intensity around 3400 could indicate the involvement of functional groups.

To investigate the effect of pH on the adsorption process of the PC-nanosorbent, the pH level of aqueous metal solutions was set on 5.5 and 8.0 and the results are summarized in Table 1. The results show that the immobilization yield of Ni (II) and Cr (VI) was modified in alkaline and acidic conditions, respectively. In fact, the pH is crucial factor in interactions of ionic molecules that affects the surface charge density of the adsorbent and the degree of metal ionization. Metal ions may proceed through: (I) chelation of metal cations on electronic doublet of N (from free amine groups) in near neutral solutions, or (II) electrostatic attraction and ion-exchange mechanisms for the removal of metal anions on protonated amine groups in acidic solutions (Benettayeb et al., 2021). The adsorption of Cr (VI) in aqueous solution was primarily driven by electrostatic interactions, due to the protonation of amino group, and some Cr (VI) ions are reduced into Cr (III) by amino group during the adsorption process (Sun et al., 2025). With the increase of pH, the PEIMNPs surfaces are increasingly deprotonated and the competition from OH^- increased, resulting in the weak interaction between Cr (VI) and adsorbents. In addition, Cr (VI) generally exists in solution as different forms of oxyanions, i.e. $HCrO^{4-}$, $CrO4^{2-}$ and $Cr_2O_7^{2-}$. For a changed to CrO_4^{2-} from $HCrO^{4-}$ at pH > 7. And the adsorption free energy of CrO_4^{2-} (− 2.1 to − 0.3 kcal mol^{-1}) is higher than that of $HCrO^{4-}$ (− 2.5 to − 0.6 kcal mol^{-1}) (Weng et al., 1997). Consequently, CrO_4^{2-} is less likely adsorbed than $HCrO^{4-}$ at the same concentration. Based on the discussion above, it was concluded that the electrostatic interaction between anionic Cr (VI) and positive charged sites on adsorbents was the predominant adsorption mechanism. As pH increases, amine surfaces become increasingly deprotonated and competition from OH^- increases, leading to a weaker interaction between Cr (VI) and the adsorbent (Chen et al., 2015). In the prepared nanosorbent, due to the presence of PEI and PC, there are both carboxylic and amine functional groups are available at the surface of the particles. Notice that, the oxygen in the carboxylate groups is considered a hard base, while the nitrogen atoms in the amine groups are classified among the intermediate bases. According to Pearson's rules, hard acids react preferentially with hard acids and soft bases with soft acids. Ni (II) metal ions are borderline acids; it is assumed that they preferentially bind to amine groups (Benettayeb et al., 2021). At low pH, due to the presence of HO^{3+}, there is competition between Ni (II) and HO^{3+}, and hydrogen ions bind better to the surface adsorption site. As pH increases, the number of protons in the solution decreases and Ni (II) has more opportunity to bind to the active sites (Wen et al., 2018). For this reason, the absorption of Ni (II) is enhanced under higher pH, where the protonation of amino groups is progressed.

Figure 5 shows the immobilization yields of Ni (II) and Cr (VI) ions obtained by the PC-nanosorbent at the different initial concentrations. The results indicate that the system could

Table 1. Investigating the effect of pH on the adsorption process

Heavy metal	pH	Y (%)	q (mg g^{-1})
Ni (II)	5.5	72.50	10.87
	7.0	83	12.45
	8.0	80.00	12.00
Cr (VI)	5.5	40.00	6.00
	7	31.00	4.65
	8	30.00	4.50

completely remove Ni (II) ions from an aqueous environment up to 50 mg L^{-1} and further increase in the initial Ni (II) concentration decreased the immobilization yield to about 80 and 40% at 200 and 1000 mg L^{-1}, respectively. However, the PC-nanosorbent particles had a weaker performance for the adsorption of Cr (VI) ions as the same conditions where the immobilization yield was 36% for 25 mg L^{-1} of Cr (VI) ions and it decrease to 20% at 1000 mg L^{-1}. The observation confirmed the PC-nanosorbent had a higher affinity for the adsorption of Ni (II). Previously, the application of a magnetic glycine-grafted chitosan for Ni (II) adsorption resulted in 50% nickel adsorption with an initial concentration of 0.3 mmol L^{-1} (17.6 mg L^{-1}) (Benettayeb et al., 2021). In one study, nickel recovery from dilute aqueous solutions (up to 0.6 mM) was performed by a complexation-ultrafiltration process with polyacrylate sodium (PAAS) and PEI, which resulted in 93% nickel removal (Shao et al., 2013). Li et al, used a type of poly(ethyleneimine)/chitosan aerogel beads to remove Cr (VI) with an initial concentration of 100 from aqueous solutions, and their results showed 80% chromium removal (Li et al., 2017). In another study, lignin spherical particles were used to remove Cr (VI) with an initial concentration of 200 mg L^{-1} using PEI as a modification strategy. The results showed a removal of 85.44% (Kwak et al., 2020). Compared to other studies, the present study has had favorable results for the removal of nickel metal, especially since the concentrations studied were higher than other studies. However, the results for chromium are lower, which the aim of the present study was selective adsorption of Ni (II) against Cr (VI) from aqueous solutions.

Further evaluations were performed by the determine adsorption capacities at the equilibrium state (q_e) and the results are presented in Figure 6 and 7 for Ni (II) and Cr (VI) ions respectively. The adsorption capacities show ascending trends for both Ni (II) and Cr (VI) ions. However, the slope of curves in Figure 6 and 7 did not remain constant with variation of the ion's concentrations and decreased with an increase in the ion's concentrations. To mathematical description the behaviors, the experimental adsorption capacities were fitted to the Langmuir isotherm model. A comparison of the best-fitted Langmuir model to the experimental data is presented in Figure 6 and 7. The following linearized form of the Langmuir model was used to determine the constants of this model:

$$\frac{1}{q_e} = \frac{1}{q_{max} \times K_L} \times \frac{1}{C_e} + \frac{1}{q_{max}} \tag{5}$$

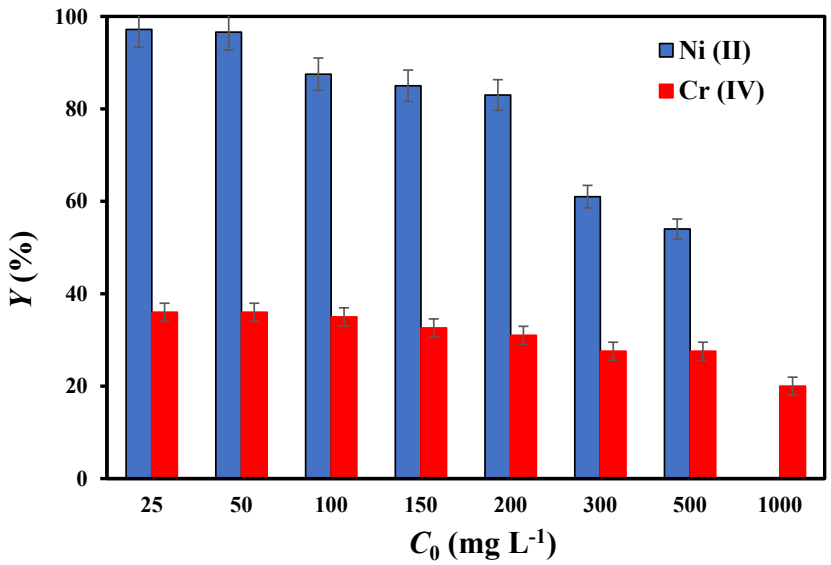

Fig. 5. Removal yield of Ni (II) and Cr (VI) ions from aqueous solutions at different initial concentrations.

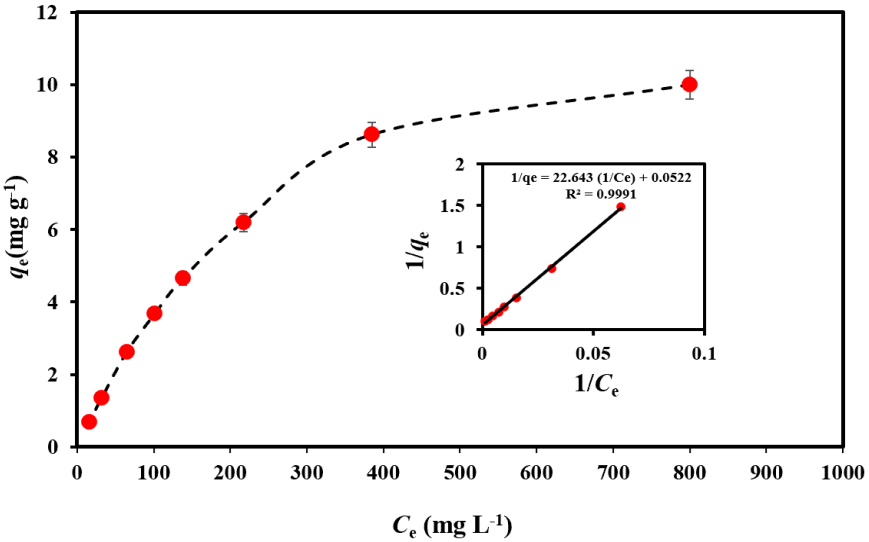

Fig. 6. Experimental qe values as a function of Ce. Insert: showed the correlation of the experimental data with linear form of Langmuir model for Ni (II) ions.

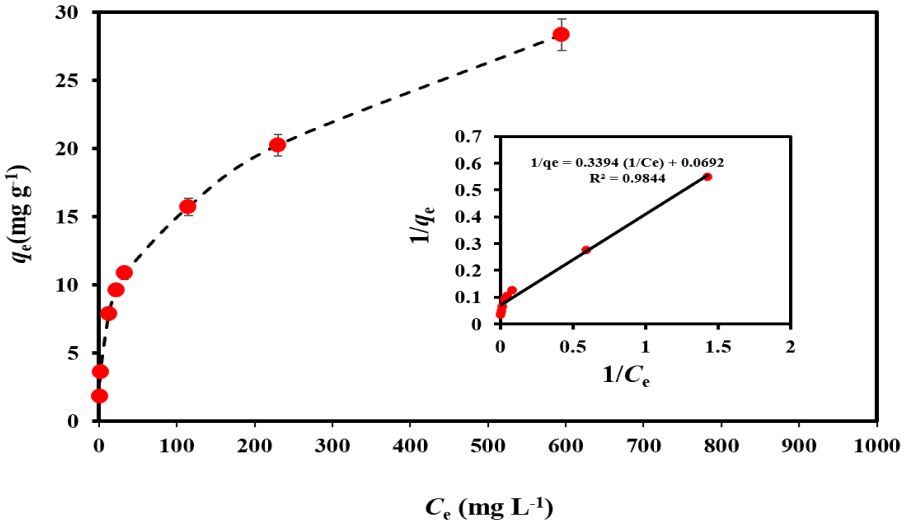

Fig. 7. Experimental qe values as a function of Ce. Insert: showed the correlation of the experimental data with linear form of Langmuir model for Cr (VI) ions.

Therefore, the plot $1/q_e$ versus $1/Ce$ obtained a straight line, from which the values of q_{max} and K_L can be calculated from the slope and intercept, respectively.

Figure 6 and 7 also showed the plot $1/q_e$ versus $1/C_e$ obtained for the systems. Both systems had high correlation coefficient ($R^2 = 0.9991$ for Ni (II) and $R^2 = 0.9844$ for Cr (VI)). It shows that the agreement between the experimental observations and the Langmuir model concepts. This model fundamentally developed through a homogeneous surface with a finite number of identical active sites. Therefore, the adsorptions of Ni (II) and Cr (VI) ions were carried out by a monolayer adsorption on nonabsorbent particles. The constants for the best-fitted Langmuir model are summarized in Table 2. Langmuir constants for the adsorption of Ni (II) were q_{max} = 19.16 mg g^{-1} and K_L = 0.0023 L mg^{-1}. Langmuir constants for Cr (VI) ions were q_{max} = 14.45 mg g^{-1} and K_L = 0.2039 L mg^{-1}.

The adsorption behavior of Ni (II) and Cr (VI) for an initial concentration of 500 mg L^{-1} was monitored during the adsorption experiments and the results are presented in Figure 8. The results showed that the adsorption of Ni (II) ions was occurred rapidly than the Cr (VI) where 51% of the initial concentration of Ni (II) ions was immobilized after 10 minutes. However, only 15.4% of the initial Cr (VI) ions was adsorbed at the same conditions. It shows a fast initial uptake for Ni (II) ions, followed by a slow approach to equilibrium. In contrast, Cr (VI) adsorption started with a lower rate and continued to reach a 54% immobilization yield as the equilibrium state after 33 hours. The results are parallel with those reported by others for the removal of chromium and nickel from electroplating wastewater using magnetite particulate adsorbent (Dube et al., 2016). It shows strong affinity and rapid surface binding to available active sites, followed by slower diffusion into less accessible sites (Su et al., 2007). Cr (VI) exhibits slower adsorption, suggesting that its interaction with the adsorbent is weaker, possibly due to electrostatic repulsion (as anionic species) or steric hindrance (Liu et al., 2023). The gradual increase in Cr (VI) removal suggests a slower adsorption mechanism, possibly due to weaker interactions with the adsorbent surface. The temporal variations of Ni (II) and Cr (VI) adsorption on the PC-nanosorbent were modelled with a pseudo-second-order kinetic expression (Naderi et al., 2018; Rout et al., 2015):

$$\frac{dq_t}{dt} = K_2\left(q_t - q_e\right)^2 \tag{6}$$

By integrating the above equation with the boundary conditions at $t = 0 \rightarrow q_t = 0$ and $t = t \rightarrow q_t = q_t$, this equation reentered as the following form (Chen et al., 2014):

$$\frac{t}{q_t} = \frac{1}{K_2\left(q_e\right)^2} + \frac{t}{q_e} \tag{7}$$

Table 2. Estimated Langmuir constants for the immobilization of Ni (II) and Cr (VI) ions.

Constant	Ni (II)	Cr (VI)
q_{max} (mg g^{-1})	19.16	14.45
K_L (L mg^{-1})	0.0023	0.2039

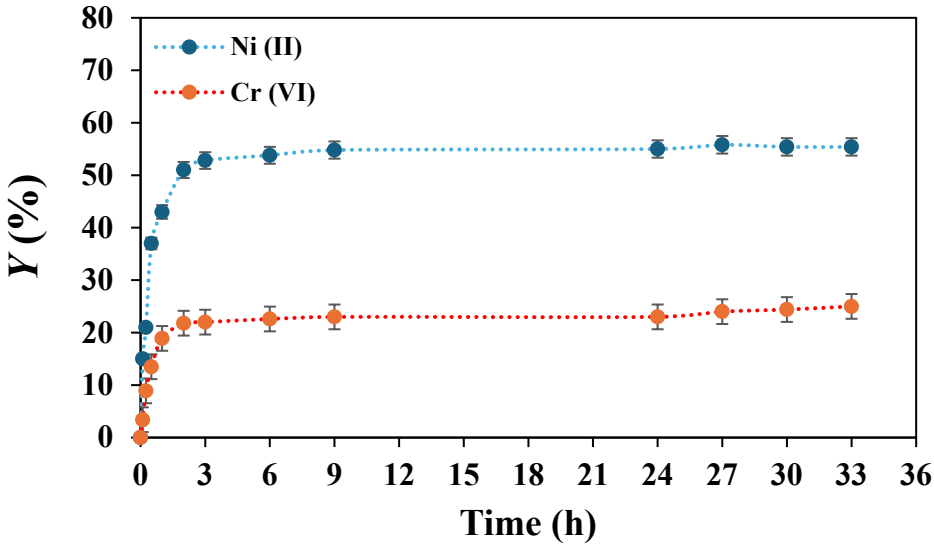

Fig. 8. Temporal variations of the immobilization yield for ions during the adsorption experiments on the PC-nano sorbents.

Where q_e is the amount of adsorbate at equilibrium (mg g^{-1}), q_t is the amount of adsorbate at time (mg g^{-1}), K_2 is the pseudo-second-order rate constant, and t is contact time (min).

A comparison between the experimental data and Equation (7) for both Ni (II) and Cr (VI) ions is presented in Figure 9. The agreement of the experiential observations and the linearized form of the pseudo-second-order kinetic model is entirely confirmed by the high value of R^2 for these systems. Table 3 shows the obtained kinetic constant for the adsorption processes. This kinetic model assumes that the adsorption rate depends on the square of the number of vacant sites on the adsorbent surface (Naderi et al., 2018; Rout et al., 2015). The constants of the pseudo-second-order kinetic model for the adsorption of Ni (II) and Cr (VI) using the PC-nanosorbent particles were q_e = 20.88 mg g^{-1} and K_2 = 0.26 g mg^1 $h^{-1}$for Ni (II) and 9.37 mg g^{-1} and 0.160 g mg^{-1} h^{-1} for Cr (VI). Previously, a magnetic nanocomposite alginate beads (PPy-NTs/PEI@Alg@NiFe2O4) were synthesized using alginate as the encapsulation reagent and polypyrrole/polyethylene imine with nano $NiFe_2O_4$ as a functional filler to remove toxic Zn^{2+} and Pb^{2+} from polluted water (Motawea et al., 2024). The optimal adsorption capacity (q_e = 18.6 mg g^{-1}) for Zn^{2+} removal was observed at pH = 6, while the optimal pH for the Pb^{2+} remediation was at pH = 4.5 with a q_e = 32.6 mg g^{-1} (Motawea et al., 2024). In addition, the data of Table 3 show that the q_e and K_2 were bigger for Ni (II) against Cr (VI). The higher rate constant (K_2) for Ni (II) indicates the adsorption of the ions was carried out faster (by 64%) versus Cr (VI) ions on the PC-nanosorbents. It is in agreement with the observations of Figure 9. Also, the differences in q_e values reflect both the number of available binding sites and the strength of interaction between each ion and the adsorbent surface. The q_e value for the adsorption of Ni (II) was upper than 2-fold of Cr (VI). It could be explained due to the tendency of Ni (II) ions for electron sharing or exchange with surface functional groups (amine, hydroxyl, or carboxyl groups).

The spent nanosorbents were regenerated using the method described previously. The results

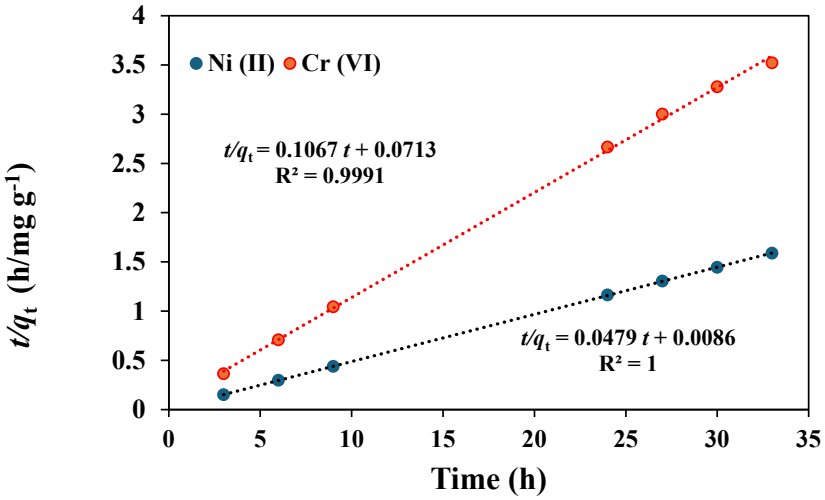

Fig. 9. Pseudo-second-order kinetic model for the immobilization of Ni (II) and Cr (VI).

Table 3. The constants of the Pseudo-second-order kinetic model for the immobilization of Ni (II) and Cr (VI) using the PC-nano sorbent particles.

Constant	Ni (II)	Cr (VI)
q_e (mg g^{-1})	20.88	9.37
K_2 (g mg^{-1} h^{-1})	0.267	0.160

Table 4. Regeneration of the used PC-nano sorbent.

Heavy metal	Y (%)		
	Cycle 1	Cycle 2	Cycle 3
Ni (II)	83	75	70
Cr (VI)	31	29	26

of the regenerated adsorbent performance are given in Table 4. As can be seen, in the third cycle, the nickel metal removal rate decreased by 12.5% and the chromium metal removal rate decreased by 16%, and overall, the efficiency of the regenerated adsorbent is acceptable.

CONCLUSION

In this study, phycocyanin-functionalized magnetic adsorbents were successfully prepared and applied for the selective removal of Ni (II) from Cr (VI) ions in aqueous solutions. FTIR and spectroscopic analyses confirmed the successful attachment of phycocyanin, introducing specific functional groups such as amines and pyrrole rings that facilitate strong coordination with nickel ions. The adsorption process was found to follow pseudo-second-order kinetics and the Langmuir isotherm model, indicating chemisorption and monolayer coverage on homogeneous sites. A key finding of this work is the distinct selectivity of the PC-nanosorbent toward Ni (II), driven by the specific chemical affinity of its protein structure for transition metal cations, in contrast to the lower uptake of anionic Cr (VI) species which is governed primarily by electrostatic interactions. This selectivity highlights the potential of the material as a targeted solution for nickel recovery rather than a general-purpose adsorbent. Furthermore, the magnetic nature of the sorbent ensures easy separation, and regeneration tests demonstrated good reusability over multiple cycles. These results suggest that PC-functionalized magnetic nanoparticles are a promising, sustainable candidate for treating industrial wastewater streams contaminated with nickel. Future work should focus on evaluating the performance of this adsorbent in real industrial effluents, investigating long-term stability under complex matrix conditions, and optimizing surface functionalization to further enhance selectivity for scaling up practical applications.

REFERENCES

Alyasi, H., Wahib, S., Tong, Y., Gomez, T., & Mahmoud, K. A. (2025). Magnetic MXene chitosan-lignosulfonate composite (Fe_3O_4@ MCLS) for the reductive removal of Cr (VI) and other heavy metals from water. J. Hazard. Mater. Adv., 17, 100536.

Anfar, Z., Amedlous, A., Majdoub, M., Ait El Fakir, A., Zbair, M., Ait Ahsaine, H., ... & El Alem, N. (2020). New amino group functionalized porous carbon for strong chelation ability towards toxic heavy metals. RSC Adv., 10(52), 31087-31100.

Antelo, F. S., Costa, J. A. V., & Kalil, S. J. (2008). Thermal degradation kinetics of the phycocyanin from *Spirulina platensis*. Biochem. Eng. J., 41(1), 43–47.

Ayalew, Z. M., Guo, X., & Zhang, X. (2022). Synthesis and application of polyethyleneimine (PEI)-based composite/nanocomposite material for heavy metals removal from wastewater: A critical review. J. Hazard. Mater. Adv., 8, 100158.

Bagdat, S., Tokay, F., Demirci, S., Yilmaz, S., & Sahiner, N. (2023). Removal of Cd (II), Co (II), Cr (III), Ni (II), Pb (II) and Zn (II) ions from wastewater using polyethyleneimine (PEI) cryogels. J. Environ. Manag., 329, 117002.

Ballav, N., Maity, A., & Mishra, S. B. (2012). High efficient removal of chromium (VI) using glycine

doped polypyrrole adsorbent from aqueous solution. Chemical Engineering Journal, 198, 536-546.
Bellamy-Carter, J., Sound, J. K., & Leney, A. C. (2022). Probing heavy metal binding to phycobiliproteins. The FEBS journal, 289(15), 4646-4656.
Benettayeb, A., Morsli, A., Elwakeel, K. Z., Hamza, M. F., & Guibal, E. (2021). Recovery of heavy metal ions using magnetic glycine-modified chitosan—application to aqueous solutions and tailing leachate. Appl. Sci., 11(18), 8377.
Chen, B., Zhao, X., Liu, Y., Xu, B., & Pan, X. (2015). Highly stable and covalently functionalized magnetic nanoparticles by polyethyleneimine for Cr (VI) adsorption in aqueous solution. RSC Adv., 5(2), 1398-1405.
Dube, D., Parekh, C. T., & Nyoni, B. (2016). Removal of chromium and nickel from electroplating wastewater using magnetite particulate adsorbent: (1) Effect of pH, contact time and dosage, (2) Adsorption isotherms and kinetics. Mod. Appl. Sci., 10(7), 222–232.
Ebrahimi, A., Pazuki, G., Mozaffarian, M., Ahsaie, F. G., & Abedini, H. (2023). Separation and purification of C-phycocyanin from spirulina platensis using aqueous two-phase systems based on triblock thermosensitive copolymers. Food Bioprocess Technol., 16(11), 2582-2597
Fang, L., Zeng, J., Wang, H., He, F., Wan, H., Li, M., ... & Luo, X. (2023). Insights into the proton-enhanced mechanism of hexavalent chromium removal by amine polymers in strong acid wastewater: Reduction of hexavalent chromium and sequestration of trivalent chromium. J. Colloid Interface Sci., 650, 515–525.
Fernández-Rojas, B., Hernández-Juárez, J., & Pedraza-Chaverri, J. (2014). Nutraceutical properties of phycocyanin. Journal of functional foods, 11, 375-392.
Gelagutashvili, E. (2013). Binding of heavy metals with C-phycocyanin: a comparison between equilibrium dialysis, fluorescence and absorption titration. Am. J. Biomed. Life Sci. 1(1), 12-16.
Hossain, M. S., & Okino, T. (2024). Cyanoremediation of heavy metals (As (V), Cd (II), Cr (VI), Pb (II)) by live cyanobacteria (*Anabaena variabilis* and *Synechocystis* sp.): an eco-sustainable technology. RSC Adv., 14(15), 10452–10463.
Hu, D., Xu, R., Jin, Y., Sun, S., Ye, J., Wu, J., ... & Lu, Y. (2024). Green and sustainable extraction of phycocyanin from Spirulina platensis by temperature-sensitive polymer-based aqueous two-phase system and mechanism study. Bioresource Technology, 407, 131142.
Karami, N., Mohammadpour, A., Samaei, M. R., Amani, A. M., Dehghani, M., Varma, R. S., & Sahu, J. (2024). Green synthesis of sustainable magnetic nanoparticles Fe_3O_4 and Fe_3O_4-chitosan derived from *Prosopis farcta* biomass extract and their performance in the sorption of lead (II). Int. J. Biol. Macromol., 254, 127663.
Kazazi, M., Afshar, A., & Sajjadnejad, M. (2013). The Inhibition Effect of Polyethylenimine (PEI) on Pitting Corrosion of 304 Austenitic Stainless Steel in 3.5% NaCl Solution.
Kwak, H. W., Lee, H., & Lee, K. H. (2020). Surface-modified spherical lignin particles with superior Cr (VI) removal efficiency. Chemosphere, 239, 124733.
Li, N., Qin, L., Jin, M., Zhang, L., Geng, W., & Xiao, X. (2021). Extracellular adsorption, intracellular accumulation and tolerance mechanisms of *Cyclotella* sp. to Cr (VI) stress. Chemosphere, 270, 128662.
Li, R., An, Q. D., Xiao, Z. Y., Zhai, B., Zhai, S. R., & Shi, Z. (2017). Preparation of PEI/CS aerogel beads with a high density of reactive sites for efficient Cr (VI) sorption: batch and column studies. RSC Adv., 7(64), 40227-40236.
Liu, B., Xin, Y.-N., Zou, J., Khoso, F. M., Liu, Y.-P., Jiang, X.-Y., ... & Yu, J.-G. (2023). Removal of chromium species by adsorption: Fundamental principles, newly developed adsorbents and future perspectives. Molecules, 28(2), 639.
Mahmud, H. N. M. E., Huq, A. O., & binti Yahya, R. (2016). The removal of heavy metal ions from wastewater/aqueous solution using polypyrrole-based adsorbents: a review. Rsc Advances, 6(18), 14778-14791.
Motawea, E. A., El-Sabban, A. O., Kang, J., & Gun Ko, Y. (2024). Efficient multifunctional PPy-NTs/PEI@alginate@NiFe2O4 magnetic beads for heavy metals removal: Experimental design and optimization interpretations, Int. J. Biol. Macromol., 282(6); 137437.
Musah, B. I., Xu, Y., Liang, C., & Peng, L. (2022). Biosorption of chromium (VI), iron (II), copper (II), and nickel (II) ions onto alkaline modified Chlorella vulgaris and Spirulina platensis in binary

systems. Environ. Sci. Pollut. Res., 29(41); 62514–62536.
Paryav, S., Rajabifar, N., Rostami, A., Abbasi, M., & Akrami, M. (2025). Assembling carbon nanotube and graphene in chitosan/sodium alginate hydrogels for ion removal applications. Polymers, 17(3), 353.
Shao, J., Qin, S., Davidson, J., Li, W., He, Y., & Zhou, H. S. (2013). Recovery of nickel from aqueous solutions by complexation-ultrafiltration process with sodium polyacrylate and polyethylenimine. J Hazard. Mat., 244, 472-477.
Shinde, D. R., Nikam, T. D., & Ghole, V. S. Utilization of biomass of nostoc species for production of pigments and adsorption of heavy metal ions Cu (II), Cd (II) and Cr (VI) from aqueous solution. Biorem., Biodiv. Bioavail., 3(1), 49-54.
Sinad, K. V. G., Peralta, M. M., Sabularse, V. C., & Lacsamana, M. S. (2021). Immobilization of phycocyanin in a rice hull nanosilica/calcium-alginate bead system for cadmium ion remediation. Philipp. J Sci., 150(3).
Sobhanardakani, S., Jafari, A., Zandipak, R., & Meidanchi, A. (2018). Removal of heavy metal (Hg (II) and Cr (VI)) ions from aqueous solutions using Fe_2O_3@ SiO2 thin films as a novel adsorbent. Process safety and environmental protection, 120, 348-357.
Su, H., Chen, S., & Tan, T. (2007). Surface active site model for Ni^{2+} adsorption of the surface imprinted adsorbent. Process Biochem., 42(4), 612–619.
Sun, X. D.; Yang, H.; Duan, Z., & Yan, K. (2025). Polyethyleneimine modified cellulose nanofiber microgel for rapid and efficient Cr (VI) removal. Cellulose, 32 (4); 2537–2551.
Tabish, M., Tabinda, A. B., Mazhar, Z., Yasar, A., Ansar, J., & Wasif, I. (2024). Physical, chemical and biological treatment of textile wastewater for removal of dyes and heavy metals. Desal. Water Treat., 320, 100842.
Tchounwou, P. B., Yedjou, C. G., Patlolla, A. K., & Sutton, D. J. (2012). Heavy metal toxicity and the environment. Mol. Clin. Environ. Toxicol., 3, 133–164.
Thevarajah, B., Nishshanka, G. K. S. H., Premaratne, M., Wasath, W. A. J., Nimarshana, P., Malik, A., & Ariyadasa, T. U. (2023). Cyanobacterial pigment production in wastewaters treated for heavy metal removal: Current status and perspectives. J. Environ. Chem. Eng., 11(1), 108999.
Thiripelu, P., Manjunathan, J., Revathi, M., & Ramasamy, P. (2024). Removal of hexavalent chromium from electroplating wastewater by ion-exchange in presence of Ni (II) and Zn (II) ions. J. Water Process Eng., 58, 104815.
Wang, C. C., & Wang, C. C. (2006). Adsorption characteristics of metal complexes by chelated copolymers with amino group. React. Func. Polymers, 66(3), 343-356.
Wang, W., Zhou, J., Achari, G., Yu, J., & Cai, W. (2014). Cr (VI) removal from aqueous solutions by hydrothermal synthetic layered double hydroxides: Adsorption performance, coexisting anions and regeneration studies. Colloids Surf. A, 457, 33–40.
Wen, X., Du, C., Zeng, G., Huang, D., Zhang, J., Yin, L., & Wan, J. (2018). A novel biosorbent prepared by immobilized Bacillus licheniformis for lead removal from wastewater. Chemosphere, 200; 173-179.
Weng, C. H., Wang, J. H., & Huang, C. P. (1997). Adsorption of Cr (VI) onto TiO2 from dilute aqueous solutions. Water science and technology, 35(7), 55-62.
Yi, C., Niu, H.-Y., Sui, L., Zhu, J.-J., Tian, Y., Niu, C.-G., ... & Huang, D.-W. (2025). A low-cost bio-based cellulose composite hydrogel with cross-linked structures for efficient capture of heavy metal ions. Sep. Purif. Technol., 358, 130213.
Zhang, C., Li, H., Sui, L., & Zhang. (2026). Efficient removal of multiple low-level heavy metals by microcrystalline cellulose-based calcium carbonate/L-cysteine doped polyethyleneimine composite MCC@CaCO3/LPEI: Performance and mechanisms, J. Environ. Chem. Eng., 14(2).